Jurnal Teknologi

Full paper

# Preparation and Photocatalytic Activity of Mixed Phase Anatase/rutile $TiO_2$ Nanoparticles for Phenol Degradation

Mohamad Azuwa Mohamed[a,b], Wan Norharyati Wan Salleh[a,b*], Juhana Jaafar[a,b], Norhaniza Yusof[a,b]

[a]*Advanced Membrane Technology Research Centre, Universiti Teknologi Malaysia, 81310 UTM Johor Bahru, Johor, Malaysia*
[b]*Faculty of Petroleum and Renewable Energy Enginneering, Universiti Teknologi Malaysia, 81310 UTM Johor Bahru, Johor, Malaysia*

*Corresponding author: hayati@petroleum.utm.my

**Article history**

Received :1 November 2013
Received in revised form :
1 June 2014
Accepted :30 June 2014

**Graphical abstract**

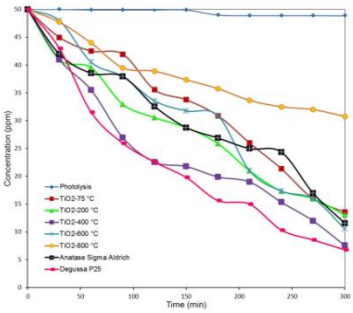


**Abstract**

The evolution of desirable physico-chemical properties in high performance photocatalyst materials involves steps that must be carefully designed, controlled, and optimized. This study investigated the role of key parameter in the preparation and photocatalytic activity analysis of the mixed phase of anatase/rutile $TiO_2$ nanoparticles, prepared via sol-gel method containing titanium-n-butoxide $Ti(OBu)_4$ as a precursor material, nitric acid as catalyst, and isopropanol as solvent. The prepared $TiO_2$ nanoparticles were characterized by means of XRD, SEM, and BET analyses, and UV-Vis-NIR spectroscopy. The results indicated that the calcination temperature play an important role in the physico-chemical properties and photocatalytic activity of the resulting $TiO_2$ nanoparticles. Different calcination temperatures would result in different composition of anatase and rutile. The photocatalytic activity of the prepared mixed phase of anatase/rutile $TiO_2$ nanoparticles was measured by photodegradation of 50 ppm phenol in an aqueous solution. The commercial anatase from Sigma-Aldrich and Degussa P25 were used for comparison purpose. The mixed phase of anatase/rutile $TiO_2$ nanoparticles (consists of 38.3% anatase and 61.7% rutile) that was prepared at 400°C exhibited the highest photocatalytic activity of 84.88% degradation of phenol. The result was comparable with photocatalytic activity demonstrated by Degussa P25 by 1.54% difference in phenol degradation. The results also suggested that the mixed phase of anatase/rutile $TiO_2$ nanoparticles is a promising candidate for the phenol degradation process. The high performance of photocatalyst materials may be obtained by adopting a judicious combination of anatase/rutile and optimized calcination conditions.

*Keywords:* Mixed phase anatase/rutile; $TiO_2$ nanoparticles; phenol degradation; calcination temperature; photocatalytic



## 1.0 INTRODUCTION

The ability to degrade organic and inorganic pollutants comes from redox environment that is generated from photoactivation, and this makes the semiconductor $TiO_2$ to be intensively utilized as a photocatalyst in wastewater treatment [1–3]. The photoactivation of $TiO_2$ photocatalyst occurs when the absorption of UV irradiation onto $TiO_2$ particles surface takes place. The UV irradiation absorption can be equal or higher than the band gap value of 3.2 eV for anatase or 3.0 eV for rutile [4, 5]. The $TiO_2$ exists in three distinct polymorphs, which are anatase, rutile (both tetragonal crystal systems), and brookite (orthorhombic crystal system) [6, 7]. Among these three $TiO_2$, anatase possesses the best photocatalytic properties, followed by rutile, and brookite.

The study on the band gap alignment of rutile and anatase $TiO_2$ has proven that the mixed phase of anatase/rutile $TiO_2$ would have synergistic effects and higher photocatalytic activity as compared to pure phase of either in anatase or rutile [4]. Degussa P25 and Aeroxide $TiO_2$ P25 are the common commercial mixed phases of anatase/rutile $TiO_2$ with 80% anatase and 20% rutile. The reason for the synergistic effects of the mixed phase of anatase/rutile $TiO_2$ nanoparticles in photocatalytic properties has still remained elusive. It is believed that the mixed phase of anatase/rutile $TiO_2$ can improve the charge carrier separation through electron trapping in rutile and reduce the electron recombination. As a result, the formation of radical species for oxidation of substrate molecules can be maintained [8].

Sol-gel is one of the most prominent methods used to prepare mixed phase of anatase/rutile $TiO_2$ nanoparticles since it provides simplicity and low equipment requirements. The preparation of $TiO_2$ from sol-gel gives some advantages, such as the production of high purity nanocrystalline through precipitation, and the flexibility to control the synthesis process [9]. There are three main chemical reagents required in the preparation of $TiO_2$ via sol-gel method, which are precursor or the starting material for Ti source, acid catalyst, and solvent as

dispersing media. The most common precursor used in the preparation of anatase nanocrystalline are titanium-n-butoxide [9–11], titanium (IV) isopropoxide [12, 13], and tetrabutyl orthotitanate [14]. The highly crystalline $TiO_2$ nanoparticles can be prepared via sol-gel, and followed by heat treatment that ranges from 0 to 600°C [11, 15]. It has been reported that the high quality of mixed phase of anatase/rutile $TiO_2$ nanoparticles, which contributes to high photocatalytic activity, can also be obtained by manipulating the types of reagents and heat treatment conditions [7, 16, 17].

Therefore, the aim of this research was to prepare a mixed phase of anatase/rutile $TiO_2$ nanoparticles with high photocatalytic properties via sol-gel method by manipulating the calcination temperature. In this study, the titanium-n-butoxide, $Ti(OBu)_4$ was used as Ti precursor, nitric acid as catalyst, and isopropanol and distilled water as the dispersing media. The photocatalytic activity of the prepared $TiO_2$ nanoparticles was evaluated by using the photodegradation of phenol in aqueous solution.

## 2.0 EXPERIMENTAL

### 2.1 Materials

In this study, titanium-n-butoxide $Ti(OBu)_4$ from Sigma-Aldrich was used as a titanium precursor. Nitric acid was used as catalyst. Isopropanol and distilled water were used as the dispersing media. The commercial $TiO_2$ that consists of Degussa P25 and pure anatase purchased from Sigma-Aldrich, was used in the control experiment. All the chemicals used were of analytical reagent grade and used as received.

### 2.2 Preparation of Titanium Dioxide ($TiO_2$) Nanoparticles

The titanium precusor ($Ti(OBu)_4$) was added dropwise in isopropanol solution and stirred until a homogenoues mixture was obtained. The mixture was then added dropwise into distilled water and vigorously stirred for several minutes. After that, the nitric acid was added into the mixture and vigorously stirred for about 30 min. The prepared mixture was aged in tight air for several days until the formation of white sol-gel was observed. The white sol-gel was then dried at 75ºC for 74 h in vacuum oven until white powder was obtained. The dried powder was ground to get fine powder and denoted as T75. In order to study the mixed phase of anatase/rutile $TiO_2$ formation, the dried sample was subjected to calcination treatment. Four new samples were prepared after they were calcined at 200, 400, 600, and 800ºC and denoted as T200, T400, T600, and T800, respectively. Calcination treatment was carried out in furnace at 5°C $min^{-1}$ heating rate for 2 h. All the samples were preserved in a dessicator until further use.

### 2.3 Characterization Methods

X-ray diffraction (XRD) was used to analyze the crystallinity of the $TiO_2$ samples. Measurements were carried out at 40 kV and 40 mA that employed a CuKα radiation at a wavelength of 0.15418 nm. The diffracted intensity was measured at the scan range of $2\theta$ = 20–80º with a scan step speed of 1 º/min. The average sizes of the crystallites of anatase and rutile were estimated with the Scherrer equation.

$$\mathbf{D} = \frac{\mathbf{K\lambda}}{\boldsymbol{\beta}\cos\boldsymbol{\theta}} \quad (1)$$

where $K$ is Scherrer constant, $K$ is 1 if the spherical shape is assumed [16]. $\beta$, $\lambda$ and $\theta$ are the full-width-at-half-maximum (FWHM) in radian [18], radiation wavelength, and the incident angle of the X-rays, respectively.

The surface morphologies of the catalyst samples were characterized by electron scanning microscopy (SEM). The surface areas were calculated by the BET single point method. The UV-Vis spectra were used to indicate the optical responses of the prepared $TiO_2$ nanoparticles at different calcination temperatures. All the optical absorption spectra of the samples were recorded in a wavelength, ranging between 200 to 600 nm, using a UV-Vis-NIR spectrophotometer Model UV-3101PC Shimadzu.

### 2.4 Photocatalytic Activity Measurements

The photocatalytic activity of the prepared $TiO_2$ nanoparticles was evaluated via degradation of 50 ppm phenol in aqueous solution. The photodegradation process was conducted in a self-designed photocatalytic reactor that consisted of 500 ml glass beaker, and was irradiated using ultraviolet (UV) lamp (Vilber Laurmat, 312 nm, 30 watt). The photocatalyst (0.8 g) was added in the 400 ml phenol solution and sonicated for 15 min. The mixture was stirred continuously with a magnetic stirrer in the dark for 30 min to achieve the adsorption/desorption equilibrium. After that, 1 mL was taken as a blank sample before irradiation. Then, the mixture was irradiated using UV lamp. Air diffuser was used to provide sufficient $O_2$ for the reaction. The suspensions (5 ml) were then collected at 30 min interval using 0.45 µm syringe filter to eliminate excess catalysts prior to analysis. The clear liquid from each suspension was subjected to UV-Vis Spectroscopy to measure the concentration change of phenol throughout the experiment. The photocatalytic activity was indicated in percentages for phenol degradation according to the following equation;

$$\text{Degradation of phenol} = \frac{\text{Ao}-\text{At}}{\text{At}} \text{ x } 100\% \quad (2)$$

where $A_o$ is the initial concentration and $A_t$ is concenration at time t (0, 30, 60, 90, 120, 150, 180, 210, 240, 270, and 300 min). A similar experiment was carried out for the commercial anatase $TiO_2$ from Sigma-Aldrich and Degussa P25. Meanwhile, a blank experiment was also carried out with direct photolysis of phenol, irradiated under UV lamp and without the presence of photocatalyst.

## 3.0 RESULTS AND DISCUSSION

### 3.1 X-ray Diffraction Pattern of the Synthesized $TiO_2$

The XRD technique is often used to identify the existence of amorphous, anatase, or rutile $TiO_2$ nanoparticles. Figure 1 shows the XRD pattern of $TiO_2$ prepared at different calcination temperatures. As presented in Figure 1, the intensity of XRD pattern of T75 was increased with the increase of the calcination temperature from 200 to 800°C. Generally, high intensity of the XRD pattern exhibited high crystallinity. Based on the XRD pattern, a summary of crystalline properties of the $TiO_2$ nanoparticles prepared at different calcination temperatures is presented in Table 1.

From Table 1, it can be seen that T75 exhibited a mixed phase of anatase/rutile $TiO_2$ at the drying stage, as low as 75°C, with the percentage of anatase and rutile produced 95% and 5%, respectively. Although the mixed phase of anatase/rutile $TiO_2$ can be formed at 75°C, the crystalinity was low. The crystalinity

of the mixed phase of anatase/rutile $TiO_2$ was enhanced gradually as a function of calcination, as clearly shown by the intensity of the diffraction peak, that had become higher and sharper. Furthermore, Figure 1 visibly shows the intensity of the diffraction peak of anatase plane at (*101*) significantly decreased, while the diffraction peak of rutile crytal plane at (*110*) increased as the calcination temperature increased.

By increasing the calcination temperature up to 800°C, the pure phase of rutile $TiO_2$ with high crystalinity was completely formed as the dissappearence of (*101*) diffraction peak was observed. Hence, it can be concluded that the phase of transition of $TiO_2$ nanoparticles depended on the calcination temperature. This phase of transition was irreversible, in other words, rutile was prohibitted to transform back into the anatase phase although the rutile was recalcined at a lower temperature. In the present work, pure and highly crystalline rutile $TiO_2$ nanaoparticles were obtained at calcination temperature of 800°C. The diffraction peak signals of the brookite phase were observed in the sample calcined at 75°C, 200°C, and 400°C at $2\theta$ of 30.77°, 30.82°, and 30.85°, respectively.

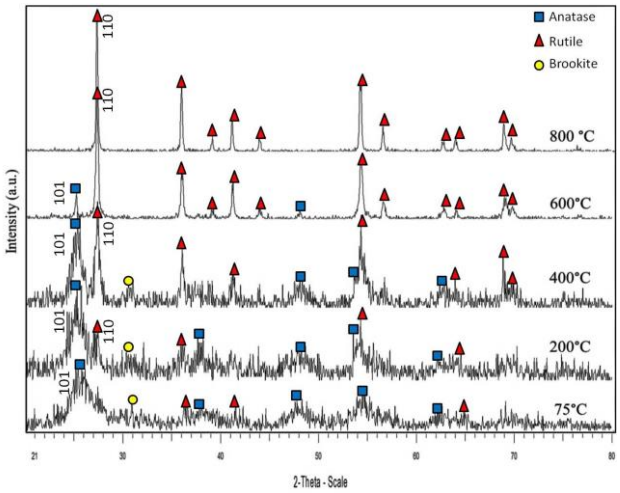


**Figure 1** XRD patterns of the $TiO_2$ nanoparticles treated at different calcination temperature

The average crystallite sizes of the anatase and rutile in each sample were estimated using the Scherrer equation. The average crystallite size estimations are tabulated in Table 1. From Table 1, the average crystallite sizes of anatase and rutile increased as calcination increased, and this result has also been found elsewhere [19]. The lowest average size of anatase crystalite was estimated at 4.3 nm, which was calcined at 75°C. As the calcination temperature increased to 200, 400, and 600°C, the average crystallite size increased to 5.7, 9.4, and 49.4 nm, respectively. Figure 1 shows that the width of the diffraction peak of anatase (*101*) at $2\theta$ = 25.4° became narrower as the calcination temperature increased from 75°C to 400°C. The same pattern of diffraction peak of $TiO_2$ rutile (110) at 2θ = 27.5° was also observed as the calcination temperature increased from 200°C to 800°C. Thus, it can be concluded that the crystallites sizes reduced as the XRD peak got broader [20].

**Table 1** Crystalline properties of the $TiO_2$ nanoparticles prepared at different calcination temperature

| Sample | Calcination Temperature (°C) | Anatase (%) | Rutile (%) | BET surface area ($m^2 g^{-1}$) | Crystalite Size (nm) | |
|---|---|---|---|---|---|---|
| | | | | | Anatase | Rutile |
| T75 | - | 95.0 | 5.0 | 204.27 | 4.3 | - |
| T200 | 200 | 52.8 | 47.2 | 200.73 | 5.7 | 24.7 |
| T400 | 400 | 38.3 | 61.7 | 73.56 | 9.4 | 30.3 |
| T600 | 600 | 12.0 | 88.0 | 27.95 | 49.4 | 35.3 |
| T800 | 800 | 0 | 100 | 2.69 | - | 56.7 |
| Anatase Sigma-Aldrich | - | 100 | 0 | 15.16 | 89.8 | - |
| Degussa P25 | - | 78 | 14 | 52.12 | 22.4 | 31.0 |

## 3.2 Scanning Electron Microscopy and BET Analysis

The morphological structure and the crystallinity of the prepared $TiO_2$ powder before and after calcination were observed by SEM. Figure 2(a) shows very fine powder and small particle size. However, as shown in Figure 2(b), the $TiO_2$ powder that was calcined at 800°C exhibited the aggregation phenomenon, which led to the formation of large $TiO_2$ particles. This was proved by the BET analysis, as shown in Table 1. It indicated that $TiO_2$ calcined at 800°C exhibited the lowest surface area of 2.69 $m^2 g^{-1}$. Meanwhile, the $TiO_2$ dried at 75°C revealed the highest surface area of 204.27 $m^2 g^{-1}$ as compared to the commercial anatase $TiO_2$ with surface area of 15.16 $m^2 g^{-1}$.

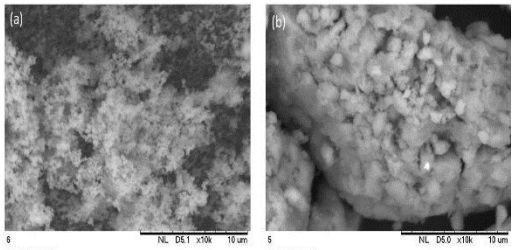


**Figure 2** SEM images of the $TiO_2$ nanoparticles: (a) $TiO_2$ dried at low temperature of 75°C (b) $TiO_2$ calcined at 800°C

## 3.3 Optical Properties

In order to study the effect of calcination temperature on optical response of prepared $TiO_2$, UV-Vis absorption spectra were characterized, as shown in Figure 3. This figure shows the UV-Vis spectrum of $TiO_2$ powder at different calcination temperatures, ranging from 75 to 800°C. It was interesting to find that the UV-Vis spectra indicated that all of the prepared $TiO_2$ obviously exhibited excellent optical responses to UV and visible region, especially sample T600. We obtained different optical responses as compared to previous studies' [12, 13, 21–25].

In the previous studies, a dopant material was introduced in the preparation of visible light active photocatalyst, such as multi wall carbon nano tubes (MWCNTs), sulphur, natural dyes, vanadium, and nitrogen. In the present study, almost all the $TiO_2$ sample prepared activated in the visible light, which might be ascribed to the *N* doping during the preparation of process due to $HNO_3$ [26]. However, as the calcination temperature

increased, the optical absorption of all the samples decreased, except T600. The strong absorbance in UV region of all the $TiO_2$ samples was due to the high tendency of electron excitation from the valence band to the conduction band. Sample T600, which consisted of 12% anatase and 88% rutile, exhibited the highest absorbance in the visible region, followed by T800, T400, T200, and T75.

From the spectrum, it could be observed that there were obvious absorbance differences in the UV light region and visible region between the samples. In the UV region, sample T600 also exhibited the highest absorbance, followed by T75, T400, T200, and T800. The highest optical absorption in both regions for T600 might be attributed to the electron affinity within the anatase and rutile phases. It has been proved that electron affinity of anatase is higher than rutile [27]. The rapid photogenerated conduction electron flows from anatase to rutile, and thus, limits the electron recombination rate [8].

The sample calcined at 800ºC showed a relatively low absorbance rate due to the increase in particles size. Previous studies have suggested that this may be attributed to the combined effect of particles size and crystallinity [11, 28]. A lower absorbance rate at the UV range led to low responses to the UV light. It can be concluded that as the particles are low in crystallinity and large in particles size, the tendency to absorb UV light is limited, which is due to the smaller surface in the limit areas [27]. The increment in calcination temperature led to this aggregation phenomenon, as shown in Figure 3, as it turned to be more severe, and roughly corresponded to the result of UV/Vis spectrum, whereby the UV responses of the samples decreased as the calcination temperature was increased.

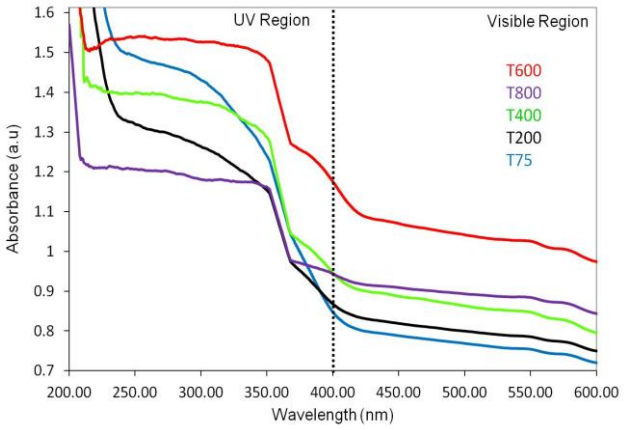


**Figure 3** UV-Vis spectrum of the $TiO_2$ nanoparticles prepared at different calcination temperature

### 3.4 Photocatalytic Activity Measurements

The photocatalytic activity of the prepared catalyst was measured by the percentage of photodegradation of phenol in aqueuos solution. The blank experiment was conducted to study the stability of phenol in aqueous solution towards UV irradiation. Figure 4 demonstrates phenol degradation in aqueous solution using $TiO_2$ nanoparticles as a function of irradiation time. The concentration of phenol decreased as the time of UV irradiation increased. Besides, it was found that after 130 min of irradiation by UV, the degradation of phenol in aqueous solution achieved 50% with samples of Degussa P25 and T400.

The direct photolysis without photocatalyst that was present in the reactor showed the lowest degradation of phenol in aqueous solution, which was only 2.3% after it was irradiated by UV at 312 nm for 180 min. This value of degradation of phenol remained unchaged as the UV irradiation time reached up to 300 min, as shown in Figure 4. From the result, it can be proved that phenol was considered stable under UV irradiation without the presence of photocatalyst.

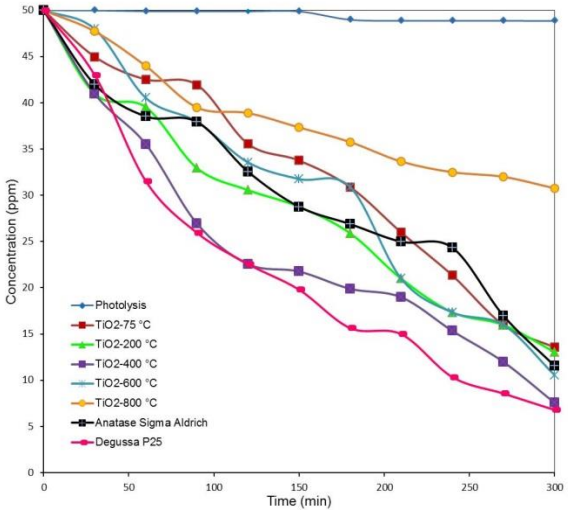


**Figure 4** The phenol degradation in aqueous solution using $TiO_2$ nanoparticles as a function of irradiation time

The summary of the photocatalytic activity for all the samples for the degradation of phenol after 300 mins are tabulated in Table 2. It was revealed that the degradation of phenol in aqueous solution by using T400 exhibited the highest photocatalytic activity. It showed that 84.88% of phenol degradation was achieved. This result is comparable with the stardard Degussa P25 by 1.54% difference in phenol degradation. Therefore, it was believed that T400 demontrated similar propeties of Degussa P25.

The lowest photocatalytic activity in the degradation of phenol, 38.48%, was obtained from T800. This was due to the low surface area created for the photodegradation reaction to take place. This result is in agreement with the UV-Vis spectroscopy data, whereby low optical response to UV was observed for the samples calcined at 800°C. A low optical response to UV leads to insuffient energy to excite electron from valence band to the conduction band [28]. The excitation of the electron is crucial since it leads to the formation of positive holes and has a positive charge [29]. This positive hole has strong oxidation power to promote the degradation of phenol molecules in aqueous solution.

**Table 2** Photocatalytic activity of the $TiO_2$ nanoparticles prepared at different calcination temperature

| Sample | Calcination Temperature (°C) | Degradation of phenol (%) after 300 min irradiation time |
|---|---|---|
| T75 | - | 72.88 |
| T200 | 200 | 73.88 |
| T400 | 400 | 84.88 |
| T600 | 600 | 78.88 |
| T800 | 800 | 38.48 |
| Anatase Sigma-Aldrich | - | 76.88 |
| Degussa P25 | - | 86.42 |
| Photolysis (control) | - | 2.3 |

In addition, the photocatalytic activity of pure anatase $TiO_2$ (referring to commercial anatase from Sigma-Aldrich) and pure rutile $TiO_2$ (referring to $TiO_2$-800ºC) can also be observed in Figure 4. As comparison to these results, the prepared mixed phase of $TiO_2$ showed higher photocatalytic activity than pure anatase and rutile $TiO_2$. Similar results could be found elsewhere [30]. The energy barrier between anatase and rutile phases facilitates the photogenerated electrons to transfer from anatase to rutile as the electron affinity of anatase is higher than rutile [4, 31]. Previous study on the band alignment of rutile and anatase $TiO_2$ indicated that the band alignment of approximately 0.4 eV drives force for the increased photocatalytic activity of anatase/rutile composites material over their individual counterparts [4]. There were significant differences in their photocatalytic activities, which were observed as the anatase phase exhibited higher photocatalytic activity than the rutile phase. Similar results were also obtained by other researcher [19].

## 4.0 CONCLUSION

The mixed phase of anatase/rutile $TiO_2$ nanoparticles was successfully prepared by using titanium-n-butoxide $Ti(OBu)_4$, nitric acid, and isopropanol as a precursor material, catalyst, and solvent, respectively. The preparation of the mixed anatase/rutile $TiO_2$ nanoparticles with controllable heating treatment had been a very simple approach and was energy saving. The effects of calcination temperature on the phsycochemical properties and photocatalytic activity were studied. The results showed that the calcination temperature played important roles in the crystallites' growth and the crystallites' phase transition in the preparation of the mixed phase of anatase/rutile $TiO_2$ nanoparticles. Based on the XRD pattern, it can be concluded that the increment in calcination temperature leads to rapid crystallites' growth and a decrease in the particles size. Furthermore, the composition of anatase decreased while rutile increased in the mixed phase of anatase/rutile $TiO_2$ as the calcination temperatures increased. On top of that, the BET analysis revealed a decrease in the $TiO_2$ surface area, which was also due to the elevated calcination temperature. From the UV-Vis spectra, all the $TiO_2$ samples prepared in the laboratory exhibited excellent optical responses to UV and visible region. The highest photocatalytic activity was demonstrated by the mixed phase of anatase/rutile $TiO_2$ nanoparticles prepared at 400ºC. The degradation of approximately 84% was achieved after 300 min of operation. This result was comparable with the photocatalytic activity obtained from the commercial anatase $TiO_2$ (Degussa P-25). The mixed phase of anatase/rutile $TiO_2$ nanoparticles prepared in this study can be used as an appropriate photocatalyst material with effective performance for phenol degradation applications.

## Acknowledgement

The authors acknowledge the support from The Ministry of Higher Education (MOHE) (Research University Grant Scheme (GUP) (Vot No: 05H08)) for funding this research project.

## References

[1] Chun, H., Yizhong, W., Hongxiao, T. 2000. Destruction of Phenol Aqueous Solution by Photocatalysis or Direct Photolysis. *Chemosphere*. 41: 1205–9.
[2] Fan, H., Li, G., Yang, F., Yang, L., Zhang, S. 2011. Photodegradation of Cellulose under UV Light Catalysed by $TiO_2$. *J Chem Technol Biotechnol*. 86: 1107–12.
[3] Manilal, V. B., Haridas, A., Alexander, R., Surender, G. D. 1992. Photocatalytic Treatment of Toxic Organics in Wastewater: Toxicity of Photodegradation Products. *Water Res.* 26: 1035–8.
[4] Scanlon, D. O., Dunnill, C. W., Buckeridge, J., Shevlin, S. A, Logsdail, A. J., Woodley, S. M., *et al.* 2013. Band Alignment of Rutile and Anatase $TiO_2$. *Nat Mater*. 12: 798–801.
[5] Ouzzine, M., Maciá-Agulló, J. A., Lillo-Ródenas, M. A., Quijada, C., Linares-Solano, A. 2014. Synthesis of High Surface Area TiO2 Nanoparticles by Mild Acid Treatment with HCl or HI for Photocatalytic Propene Oxidation. *Appl Catal B Environ*. 154–155: 285–93.
[6] Devilliers, D. 2006. Semiconductor Photocatalysis : Still an Active Research Area Despite Barriers to Commercialization. *Energeia*. 17: 1–6.
[7] Wu, Q., Wu, Z., Li, Y., Gao, H., Piao, L., Zhang, T., *et al*. 2012. Controllable Synthesis and Photocatalytic Activity of Anatase $TiO_2$ Single Crystals with Exposed {110} Facets. *Chinese J Catal.* 33: 1743–53.
[8] Ohtani, B., Prieto-Mahaney, O. O., Li, D., Abe, R. 2010. What is Degussa (Evonik) P25? Crystalline Composition Analysis, Reconstruction from Isolated Pure Particles and Photocatalytic Activity Test. *J Photochem Photobiol A Chem.* 216: 179–82.
[9] You, Y. F., Xu, C. H., Xu, S. S., Cao, S., Wang, J. P., Huang, Y. B., *et al*. 2014. Structural Characterization and Optical Property of $Tio_2$ Powders Prepared by the Sol–Gel Method. *Ceram Int.* 40: 8659–66.
[10] Ao, Y., Xu, J., Fu, D., Shen, X., Yuan, C. 2008. Low Temperature Preparation of Anatase $TiO_2$-coated Activated Carbon. *Colloids Surfaces A Physicochem Eng Asp*. 312: 125–30.
[11] Li, S., Ye, G., Chen, G. 2009. Low-Temperature Preparation and Characterization of Nanocrystalline Anatase $TiO_2$. *J Phys Chem C*. 113: 4031–7.
[12] Cimieri, I., Poelman, H., Ryckaert, J., Poelman, D. 2013. Novel Sol–gel Preparation of V-$TiO_2$ Films for the Photocatalytic Oxidation of Ethanol in Air. *J Photochem Photobiol A Chem*. 263: 1–7.
[13] Ananth, S., Arumanayagam, T., Vivek, P., Murugakoothan, P. 2014. Direct Synthesis of Natural Dye Mixed Titanium Dioxide Nano Particles By Sol–gel Method for Dye Sensitized Solar Cell Applications. *Opt - Int J Light Electron Opt.* 125: 495–8.
[14] You, Y., Zhang, S., Wan, L., Xu, D. 2012. Preparation of Continuous $TiO_2$ Fibers by Sol–Gel Method and Its Photocatalytic Degradation on Formaldehyde. *Appl Surf Sci.* 258: 3469–74.
[15] Liu, X. 2012. Preparation and Characterization of Pure Anatase Nanocrystals by Sol–gel Method. *Powder Technol.* 224: 287–90.
[16] Bakardjieva, S., Šubrt, J., Štengl, V., Dianez, M. J., Sayagues, M. J. 2005. Photoactivity of Anatase–rutile $TiO_2$ Nanocrystalline Mixtures Obtained by Heat Treatment of Homogeneously Precipitated Anatase. *Appl Catal B Environ*. 58: 193–202.
[17] Mahshid, S., Askari, M., Sasani, Ghamsari, M., Afshar, N., Lahuti, S. 2009. Mixed-phase $TiO_2$ Nanoparticles Preparation Using Sol–gel Method. *J Alloys Compd*. 478: 586–9.
[18] Moharram, A. H., Mansour, S. A., Hussein, M. A., Rashad, M. 2014. Direct Precipitation and Characterization of ZnO Nanoparticles. *J Nanomater*. 2014: 1–5.
[19] Li, Z., Liu, R., Xu, Y. 2013. Larger Effect of Sintering Temperature Than Particle Size on the Photocatalytic Activity of Anatase $TiO_2$. *J Phys Chem C*. 117: 24360–7.

[20] Ao, Y., Xu, J., Fu, D., Shen, X., Yuan, C. 2008. Low Temperature Preparation of Anatase $TiO_2$-coated Activated Carbon. *Colloids Surfaces A Physicochem Eng Asp*. 312: 125–30.
[21] Wang, W., Serp, P., Kalck, P., Faria, J. L. 2005. Visible light Photodegradation of Phenol on MWNT-$TiO_2$ Composite Catalysts Prepared by a Modified Sol–gel Method. *J Mol Catal A Chem*. 235: 194–9.
[22] Zhang, J. Y., Boyd, I.W., O'Sullivan, B. J., Hurley, P. K., Kelly, P. V., Sénateur, J. P. 2002. Nanocrystalline $TiO_2$ Films Studied by Optical, XRD and FTIR Spectroscopy. *J Non Cryst Solids*. 303: 134–8.
[23] Ruzimuradov, O., Nurmanov, S., Hojamberdiev, M., Prasad, R. M., Gurlo, A., Broetz, J., *et al*. 2014. Fabrication of Nitrogen-doped $Tio_2$ Monolith with Well-defined Macroporous and Bicrystalline Framework and Its Photocatalytic Performance Under Visible Light. *J Eur Ceram Soc*. 34: 809–16.
[24] Zhang, Q., Wang, J., Yin, S., Sato, T., Saito, F. 2004. Synthesis of a Visible-Light Active TiO 2 □ x S x Photocatalyst by Means of Mechanochemical Doping. *Journal of the American Ceramic Society*. 1163: 1161–3.
[25] Ohno, T. 2004. Preparation of Visible Light Active S-doped TiO2 Photocatalysts and Their Photocatalytic Activities. *Water Sci Technol*. 49: 159–63.
[26] Chen, Q., Liu, H., Xin, Y., Cheng, X. 2013. $TiO_2$ nanobelts–Effect of Calcination Temperature on Optical, Photoelectrochemical and Photocatalytic Properties. *Electrochim Acta*. 111: 284–91.
[27] Li, S., Ye, G., Chen, G. 2009. Low-Temperature Preparation and Characterization of Nanocrystalline Anatase $TiO_2$. *J Phys Chem C*. 113: 4031–7.
[28] Devilliers, D. 2006. Semiconductor Photocatalysis : Still an Active Research Area Despite Barriers to Commercialization. *Energeia*. 17: 1–6.
[29] Fujishima, A., Rao, T. N., Tryk, D. A. 2000. Titanium dioxide photocatalysis. *J Photochem Photobiol C Photochem Rev*. 1: 1–21.
[30] Luttrell, T., Halpegamage, S., Tao, J., Kramer, A., Sutter, E., Batzill, M. 2014. Why is anatase a better photocatalyst than rutile?--Model studies on epitaxial $TiO_2$ films. *Sci Rep*. 4: 4043.
[31] Zhang, Y., Chen, J., Li, X. 2010. Preparation and Photocatalytic Performance of Anatase/Rutile Mixed-Phase $TiO_2$ Nanotubes. *Catal Letters*. 139: 129–33.